JOURNAL OF AIRCRAFT
Vol. 46, No. 4, July–August 2009

Performance and Design Investigation of Heavy Lift Tilt-Rotor with Aerodynamic Interference Effects

Hyeonsoo Yeo* and Wayne Johnson†
NASA Ames Research Center, Moffett Field, California 94035

DOI: 10.2514/1.40102

Performance calculations were conducted for 146,600 lb conventional and quad tilt-rotors, which are to cruise at 300 kt at a 4000 ft/95°F condition. Aerodynamic interference effects on the aircraft cruise performance were quantified. Aerodynamic interference improves the aircraft lift-to-drag ratio of the baseline conventional tilt-rotor. However, interference degrades the aircraft performance of the baseline quad tilt-rotor, mostly due to the unfavorable effects from the front wing to the rear wing. A parametric study was conducted to understand the effects of design parameters on the performance of the aircraft. A reduction in rotor tip speed increased the aircraft lift-to-drag ratio the most among the design parameters investigated.

Nomenclature

A	=	rotor disk area (all rotors)
C_W	=	rotor weight coefficient, $W/\rho A(\Omega R)^2$
$L/D_e = WV/P$	=	aircraft effective lift-to-drag ratio
P	=	aircraft power
q	=	dynamic pressure
R	=	rotor radius
S	=	wing area (all wings)
V	=	flight speed
W	=	gross weight
W/A	=	disk loading
W/S	=	wing loading
ρ	=	air density
σ	=	solidity (thrust weighted total blade area/A)
Ω	=	rotor rotational speed

Introduction

THE recent NASA Heavy Lift Rotorcraft Systems Investigation [1] and ongoing Joint Heavy Lift Concept Design and Analysis have renewed interest in heavy lift aircraft for both civil and military applications. A tilt-rotor aircraft configuration has the potential to combine a vertical takeoff and landing capability with efficient, high-speed cruise flight. Accurate prediction of aircraft performance is essential for the design of future rotorcraft. It is necessary to incorporate rotor/rotor, rotor/wing, and wing/wing interference effects in the performance calculations. The advent of a quad tilt-rotor (two wings and four rotors) has increased the importance of aerodynamic interference.

There have been many studies on the aerodynamic interactions between rotor and wing of a conventional tilt-rotor in hover due to a significant wing download and its implication on hover performance [2–5]. These experimental studies have revealed the complex flow features in the proximity of the wing and rotor system. A small-scale experiment showed that geometry variations, such as the distance between the rotor and wing, wing incidence angle, wing flap angle, and rotor rotational direction, had a significant effect on the wing download [3]. Devices were developed and tested to reduce tilt-rotor download. A full-scale evaluation of the download reduction devices showed an increase in hover lift capability between 2.5 and 3.5% [4]. After Bell Helicopter proposed the development of the quad tilt-rotor (QTR) [6], researchers conducted both experiments [7,8] and analyses using computational fluid dynamics (CFD) [9,10]. Radhakrishnan and Schmitz [7,8] acquired rotor performance and airframe download data by testing a simplified 0.031-scale model of a QTR aircraft in hover and low-speed forward flight, in and out of ground effect. Gupta and Baeder [9,10] simulated flowfield around a simplified QTR vehicle using computational fluid dynamics and obtained detailed loading variations on the wings. Because the QTR is a relatively new concept, a parametric study has not been found in the open literature.

It is known that the direction of rotor rotation has a measurable effect on aircraft performance through interference between the rotor and the wing. Consequently, all tilt-rotors have been designed to take advantage of favorable interference, by using the appropriate rotation direction (inboard blades upward). However, there is little information from previous work available on the actual magnitude of interference, especially for advanced tilt-rotor configurations. The importance of overall aircraft efficiency to the viability of large tilt-rotor designs and current considerations of alternative tilt-rotor configurations, such as the quad tilt-rotor, are the motivations for the present work. The objective of the work presented here is to quantify the effect of rotor-wing aerodynamic interference on the overall cruise performance of representative large tilt-rotor configurations and to explore the sensitivity of the interference to typical design variables of a large transport tilt-rotor.

Tilt-Rotor Modeling and Analysis

The baseline conventional tilt-rotor considered is a 20 ton payload tilt-rotor, which is to cruise at 300 kt at a 4000 ft/95°F condition. The configuration of the baseline tilt-rotor is shown in Fig. 1. The aircraft has two four-bladed tilting rotors at the wing tips, a high wing, and a horizontal tail. The basic size of the aircraft was determined using the U.S. Army Aeroflightdynamics Directorate's design code RC [11]. Aircraft performance was calculated with the comprehensive rotorcraft analysis CAMRAD II [12], which has demonstrated good performance and airload correlation with test data [13].

CAMRAD II is an aeromechanics analysis of rotorcraft that incorporates a combination of advanced technologies, including multibody dynamics, nonlinear finite elements, and rotorcraft aerodynamics. The CAMRAD II aerodynamic model for the rotor blade is based on lifting-line theory using steady two-dimensional airfoil characteristics and a vortex wake model. A recent study showed that coupled CFD/rotorcraft computational structural dynamics (CSD) analyses overcame the limitations of the conventional lifting-line

Received 28 July 2008; revision received 11 December 2008; accepted for publication 16 February 2009.

*Research Scientist, Aeroflightdynamics Directorate, U.S. Army Research, Development, and Engineering Command, Mail Stop 215-1; hyeonsoo.yeo@us.army.mil. Member AIAA.

†Research Scientist, Aeromechanics Branch, Mail Stop 243-12. Fellow AIAA.

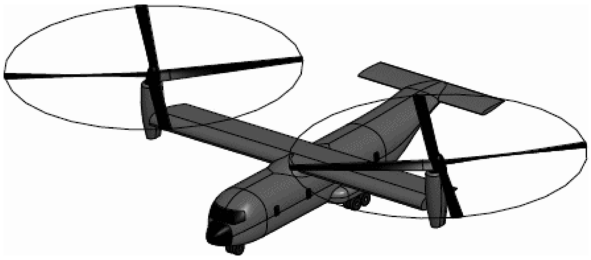

Fig. 1 Baseline tilt-rotor configuration (courtesy Gerardo Nunez, Aeroflightdynamics Directorate, U.S. Army).

aerodynamics used in rotorcraft comprehensive codes [14]. However, comprehensive analysis codes are much more computationally efficient than any equivalent CFD/CSD codes. CAMRAD II is, therefore, a very useful tool for rotorcraft research, design, and development, for which efficient aeromechanics analysis is needed.

The characteristics of the baseline tilt-rotor are summarized in Table 1. The baseline aircraft design parameters are disk loading of $W/A = 15$ lb/ft^2, blade loading of $C_W/\sigma = 0.14$, and wing loading of $W/S = 100$ lb/ft^2. The airframe and wing parasite drag is $D/q = 55$ ft^2. This drag value is considered aggressive in terms of rotorcraft trends but achievable from good fixed-wing aerodynamic design practice. A hingeless rotor hub was used, with a first blade flap frequency of 1.105/rev. The rotor was modeled as a rigid blade with a flap hinge. Wing and airframe elastic motion was not considered. The rotors rotate with the top blades moving outward in airplane mode.

The baseline quad tilt-rotor was developed (not designed by the design code RC) from the baseline conventional tilt-rotor, and had the same gross weight, disk loading, and airframe size. The configuration of the baseline quad tilt-rotor is shown in Fig. 2. The characteristics of the baseline quad tilt-rotor are summarized in Table 2. The rotor size was determined to maintain the same disk loading as the baseline conventional tilt-rotor. The front wingspan followed from maintaining the same clearance between the two rotors, and the front wing chord was determined by maintaining the same aspect ratio as the baseline conventional tilt-rotor wing. The rear wingspan was chosen as 40% larger than the front wingspan. The rear wing chord was chosen to have the same chord (15.21 ft) as the front wing from the tips to the middle of the semispan and then linearly increased to 17.35 ft at the centerline. The quarter chord line of the rear wing was kept straight. This design approach resulted in wing loading of $W/S = 67.16$ lb/ft^2. The rear rotors and wing are located 5.02 ft above the front rotors and wing. The blade structural properties were scaled to have the same first blade flap frequency as the conventional tilt-rotor (1.105/rev). The rotors rotate with the top blades moving outward in airplane mode.

Performance calculations were conduced at the design cruise of 300 kt at a 4000 ft/95°F condition. Rotor/rotor, rotor/wing, and wing/wing interferences were accounted for using the vortex wake

Table 1 Characteristics of baseline tilt-rotor design

Mission gross weight, lb	146,600
Cruise speed, kt	300
Rotor diameter, ft	78.88
Disk loading W/A, lb/ft^2	15
C_W/σ (geometric)	0.140
C_W/σ (thrust weighted)	0.154
Tip speed, ft/s	750/626
Solidity (geometric)	0.0989
Number of blades	4
Blade chord at 75%R, ft	2.79
Blade taper ratio	0.7
Aircraft drag D/q, ft^2	55.0
Wing loading, lb/ft^2	100
Wing area, ft^2	1466
Wingspan, ft	96.4

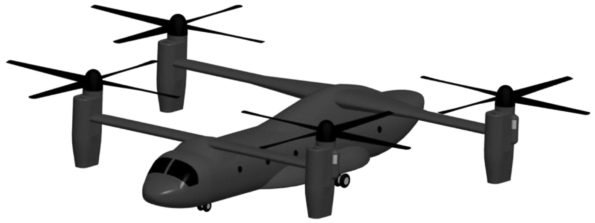

Fig. 2 Baseline quad tilt-rotor configuration (courtesy Gerardo Nunez, Aeroflightdynamics Directorate, U.S. Army).

model. The current analysis does not include a fuselage model, which is known to be important for oscillatory interference of wing on rotor, but not usually necessary for wing mean induced drag. No nacelle model was considered; thus, any end plating effect was neglected. Typical wake geometries and blade and wing lift distributions for the baseline conventional and quad tilt-rotors are shown in Figs. 3 and 4, respectively. Only the tip vortices, which dominate the interference, are drawn in these figures, but there was a full vortex lattice behind each blade and wing. The wing wake model consists of vortex lattice in the near wake behind the wing with 32 aerodynamic panels, rolling up to tip vortices (with shed wake panels between) in the far wake that interferes with the rotors and other wing. Thus, comparable models were used for both wing and rotor wakes in this investigation of the interference. A constant vortex core radius of 20% chord ($0.2c$) was used for both the conventional and quad tilt-rotors. The effects of vortex core size on the aircraft performance is discussed in a later section.

For the conventional tilt-rotor, the aircraft was trimmed using longitudinal stick (connected to the elevator), governor, and pitch attitude to obtain longitudinal and vertical force and pitching moment equilibrium of the aircraft. For some cases, rotor flapping was also trimmed to zero using rotor cyclic pitch to reduce loads; thus, there were three or seven trim variables for cruise.

For the quad tilt-rotor, the aircraft was trimmed using governor and front and rear wing pitch angles. The governor was used to achieve longitudinal force equilibrium, and the front and rear wing pitch angles were used for each wing to carry half the gross weight. Rotor flapping was also trimmed to zero using rotor cyclic pitch; thus, there were 11 trim variables for cruise.

Performance and Design Analysis

Conventional Tilt-Rotor

Performance results for the conventional tilt-rotor at the design cruise of 300 kt at a 4000 ft/95°F condition are shown here. The performance was calculated using nonuniform inflow with prescribed wake geometry. Figures 5–7 show the interference effects on the wing for the baseline configuration. The interference velocity from the rotors on the wing is shown in Fig. 5. The interference varied

Table 2 Characteristics of baseline quad-tilt-rotor design

Mission GW, lb	146,600
Cruise speed, kt	300
Rotor diameter, ft	55.78
Disk loading W/A, lb/ft^2	15
C_W/σ (geometric)	0.140
C_W/σ (thrust weighted)	0.154
Tip speed, ft/s	750/626
Solidity (geometric)	0.0989
Number of blades	4
Blade chord, 75%R, ft	1.97
Blade taper ratio	0.7
Aircraft drag D/q, ft^2	60.3
Wing loading, lb/ft^2	67.2
Front wing area, ft^2	848
Rear wing area, ft^2	1335
Front wingspan, ft	73.3
Rear wingspan, ft	102.6

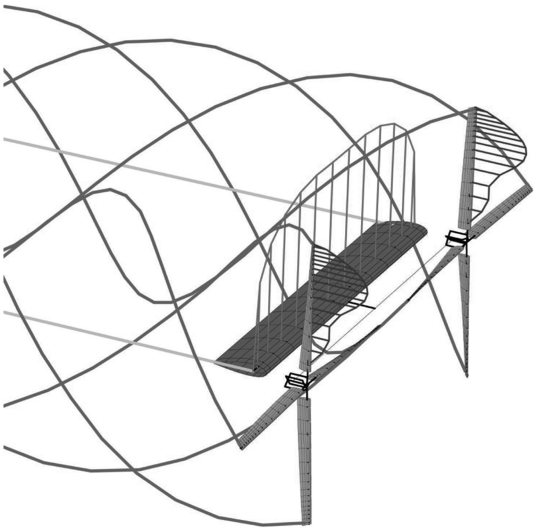

Fig. 3 Wake geometry of conventional tilt-rotor.

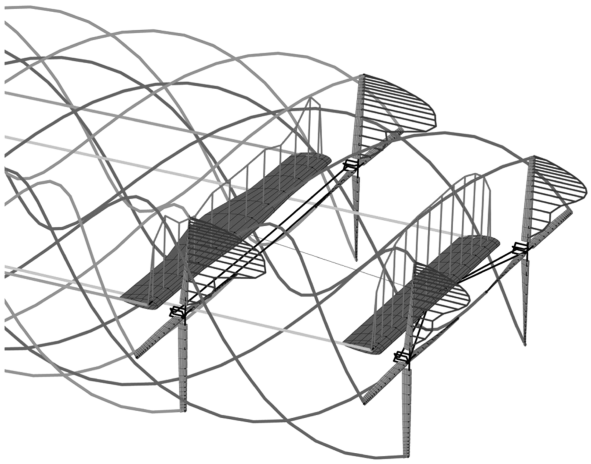

Fig. 4 Wake geometry of quad tilt-rotor.

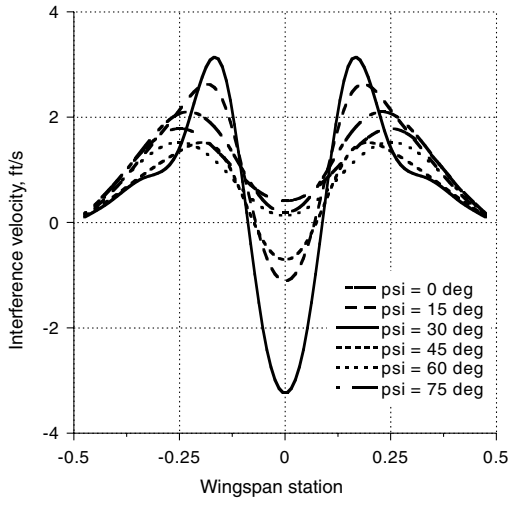

Fig. 5 Interference velocity on the wing of the conventional tilt-rotor (positive upward).

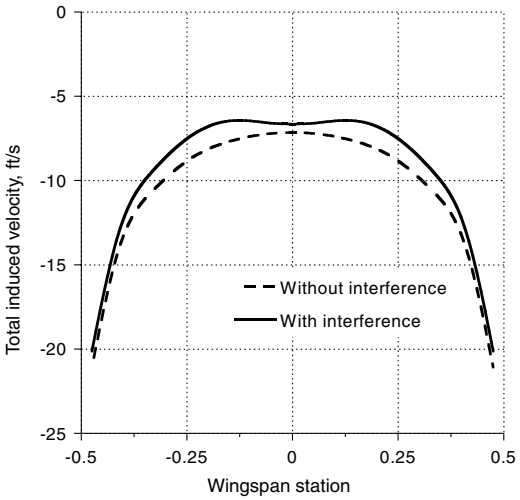

Fig. 6 Total wing induced velocity of the conventional tilt-rotor (positive upward).

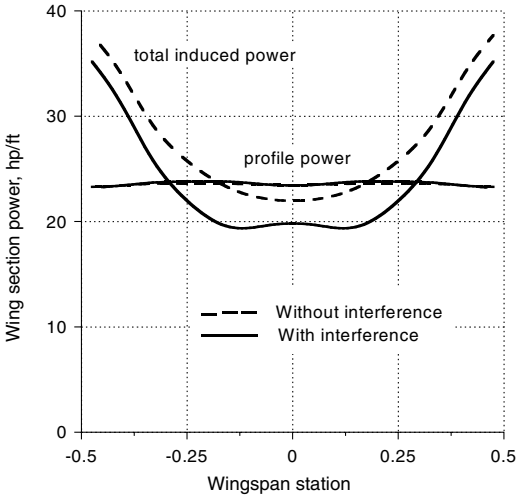

Fig. 7 Wing section power of the conventional tilt-rotor.

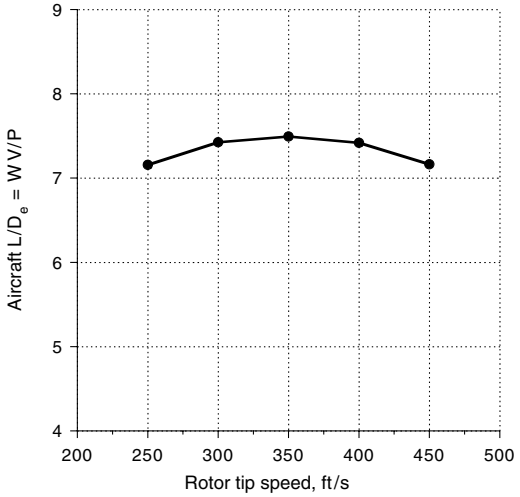

Fig. 8 Aircraft lift-to-drag ratio with rotor tip speed.

with rotor azimuth and exhibited a 4/rev variation due to the four-bladed rotors. It should be noted that rotor azimuth angle is defined as zero when the blade is pointing downstream in helicopter mode. The maximum interference was observed at a 30 deg azimuth angle, at which the blade tip vortex of the rotor passes the wing quarter chord line. These interference velocities reduce total induced velocity along the wingspan, as shown in Fig. 6. Without interference, the induced-velocity distribution is the same as that of a fixed wing. The interference has a beneficial effect on the wing performance, reducing wing induced power, as shown in Fig. 7. The interference

Table 3 Parametric variations of conventional tilt-rotor

Case 1 (C1)	Change of rotor rotational direction
Case 2 (C2)	Increase in disk loading (reduction in rotor blade radius by 5%)
Case 3 (C3)	Reduction in cruise rotor tip speed to 350 ft/s
Case 4 (C4)	Reduction in wing angle of attack by 3 deg
Case 5 (C5)	Increase in wingspan by 10%
Case 6 (C6)	Increase in wingspan by 10% and rotors move to the wing tip
Case 7 (C7)	Increase in wingspan by 10%, rotors move to the wing tip, and increase in rotor blade radius by 12.2%

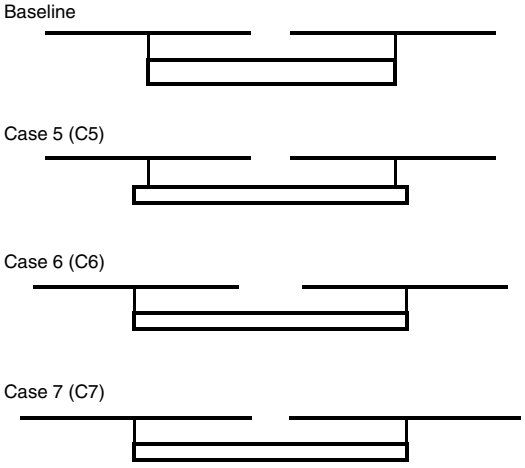

Fig. 9 Rotor and wing geometry variations for the conventional tilt-rotor.

effect did not change wing profile power. This observation, the reduction in wing drag due to favorable rotor swirl provided by up-inboard rotating rotors, was also reported in [5,15].

Figure 8 shows the aircraft lift-to-drag ratio at the cruise of 300 kt. The rotor tip speed was varied from 250 to 450 ft/s, and the optimum cruise performance was found at a 350 ft/s tip speed. Further reductions in rotor rotational speed did not improve the aircraft lift-to-drag ratio. The tip speed value of 350 ft/s was chosen for a parametric study discussed next.

A parametric study was conducted to understand the effects of design parameters on the performance of the aircraft. Table 3 shows the design parameters investigated, and the rotor and wing geometry variations are illustrated in Fig. 9. Selected parameters are expected to be available design choices. The amount of variations (e.g., 10%) was based on the typical range in design study, although a larger variation would show more dramatic effects. The first case was the change of rotor rotational direction. The second case was the increase in disk loading to 16.6 lb/ft^2 (reduction in rotor blade radius by 5%). To maintain the same blade loading, the blade chord was increased

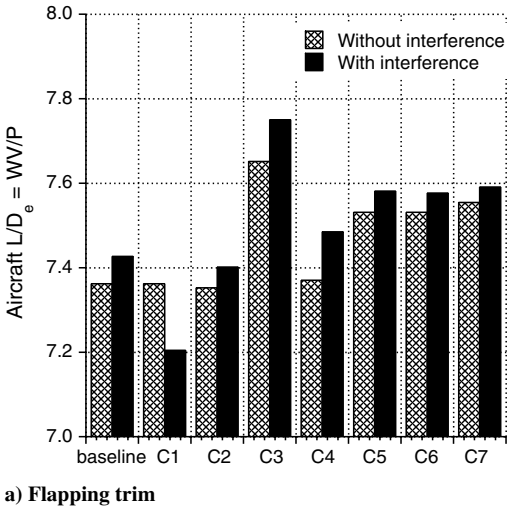

a) Flapping trim

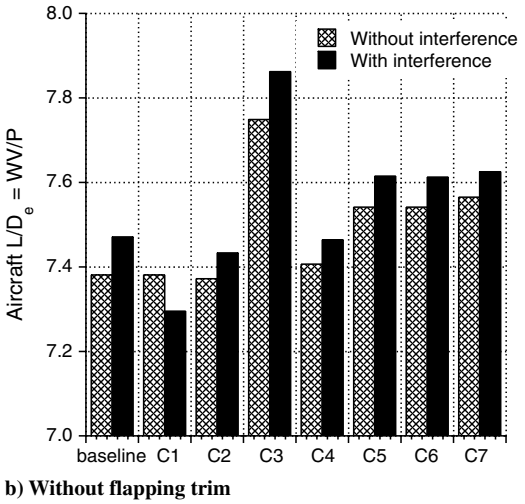

b) Without flapping trim

Fig. 10 Aircraft lift-to-drag ratio of the conventional tilt-rotor.

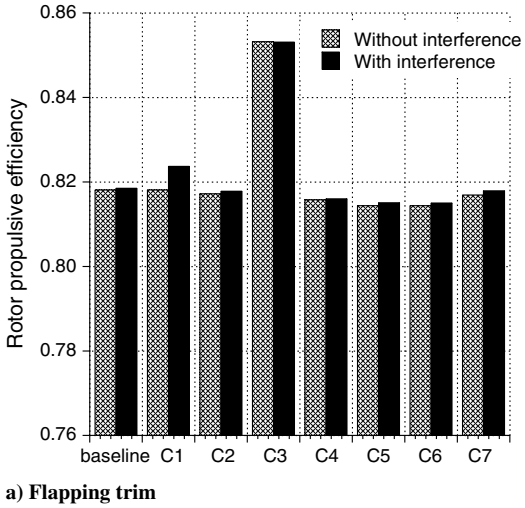

a) Flapping trim

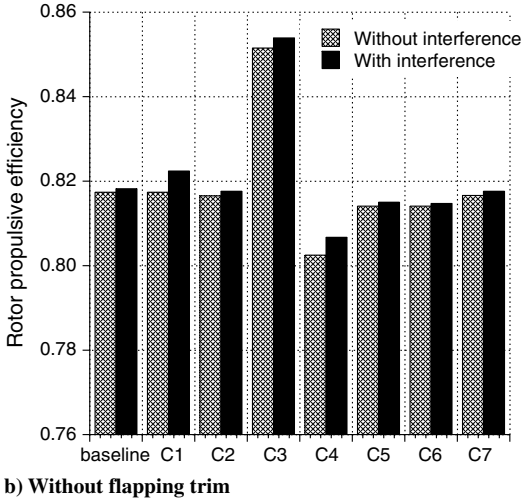

b) Without flapping trim

Fig. 11 Rotor propulsive efficiency of the conventional tilt-rotor.

accordingly. The third case was a reduction in cruise tip speed to 350 ft/s to increase the propulsive efficiency of the rotor. The fourth case was the reduction in the wing angle of attack relative to the fuselage (thus, relative to the rotors) to investigate the effect of lift sharing between rotor and wing. The fifth case was the increase in wingspan. To maintain the same wing loading, the wing chord was reduced accordingly. In this case, the rotors stay at the same wingspan as the baseline. The sixth case was the increase in wingspan, as in the fifth case, but the rotors moved to the wing tips. The seventh case was the increase in wingspan and rotor blade radius (decrease in disk loading to 11.9 lb/ft^2) and the rotors at the wing tips. To maintain the same blade loading, blade chord was decreased accordingly.

Figure 10 shows the performance results in terms of aircraft lift-to-drag ratio $L/D_e = WV/P$, calculated without accessory or other losses, all for the design cruise condition of 300 kt. Rotor/rotor and rotor/wing interferences were accounted for by using a vortex wake model for both the rotor and the wing, and the performance results with interference effects are compared with those without interference effects. Two trim strategies were used: with flapping trim and without flapping trim. The interference effects changed the aircraft lift-to-drag ratio by up to 2.1% for the parametric variations investigated. The reduction in rotor tip speed (C3) increased the aircraft lift-to-drag ratio the most, and the increase in wingspan (C5) also had a beneficial effect. The change of rotor rotational direction (C1) decreased the aircraft lift-to-drag ratio significantly, and this effect can only be observed with interference included in the calculation. The total effect of changing the rotor direction of rotation was −3.0% of L/D. The rotor disk loading change (C2, and C7 compared with C6) had a small influence on the aircraft cruise performance. In general, flapping trim reduces the aircraft lift-to-drag ratio by up to 1.4%.

Figures 11 and 12 show the rotor propulsive efficiency and wing drag (induced + parasite), respectively. These are the same calculations as in Fig. 10, except that individual performance components are compared. For the baseline case, there is a significant reduction in the wing induced drag because of the favorable combination of the rotor wake and the wing and a slight increase in rotor propulsive efficiency because of the nonuniform flowfield from the wing interference. The change of rotor rotational direction increased rotor propulsive efficiency somewhat. However, it also increased the wing induced drag significantly; thus, an overall performance penalty was observed. The reduction in rotor tip speed (C3) increased the rotor propulsive efficiency as well as decreased the wing drag. Thus, the most performance improvement was obtained. Again, the tip speed value of 350 ft/s was selected based on the optimum aircraft performance, as shown in Fig. 8. The reduction in the wing angle of attack (C4) changed lift sharing between the rotor and wing, reducing the wing lift by about 4000 lb and increasing rotor lift by about 4000 lb, although not shown in the paper. The reduced wing lift decreased the wing induced drag, and the increased rotor lift increased the rotor-induced drag. However, the reduced wing angle of attack also changed the wing tip vortex trajectories in a way that increased beneficial interference effects; thus, the rotor propulsive efficiency was not changed much. The net effect of the reduction in

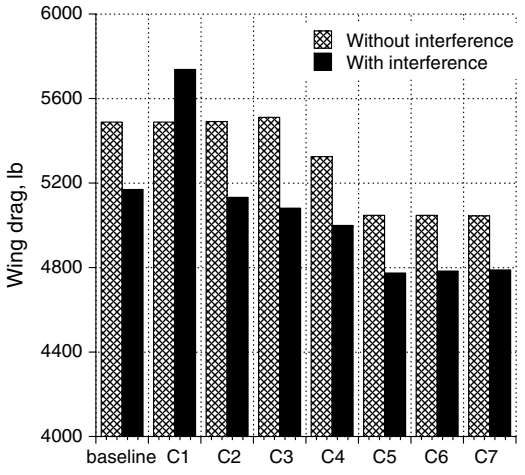

a) Flapping trim

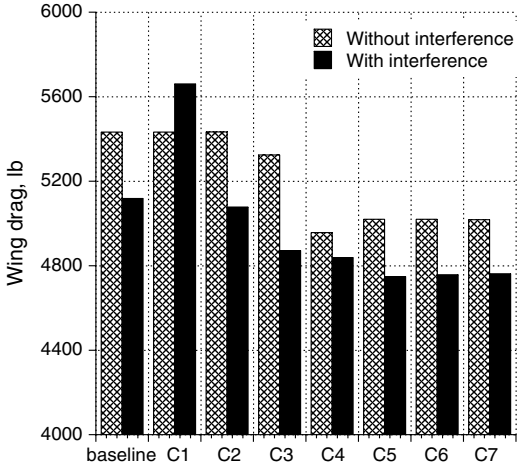

b) Without flapping trim

Fig. 12 Wing drag of the conventional tilt-rotor.

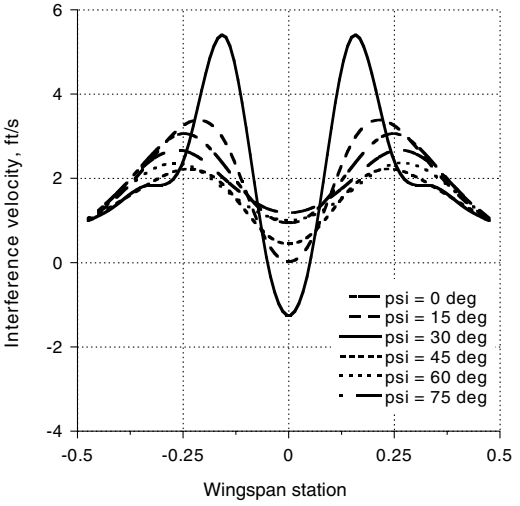

a) Front wing

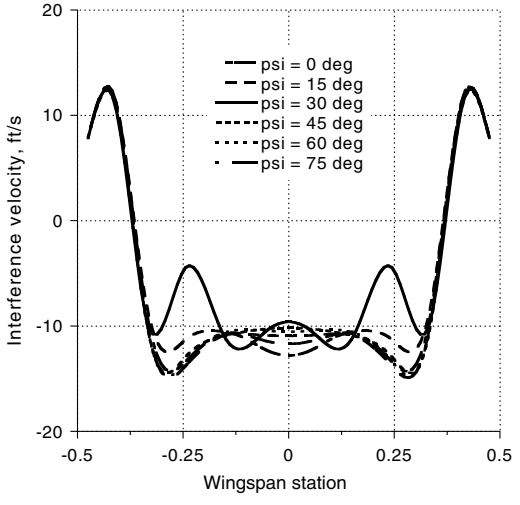

b) Rear wing

Fig. 13 Interference velocity on the wing of the quad tilt-rotor (positive upward).

wing angle of attack was a performance improvement. The increase in wingspan (C5, and decrease of wing chord) decreased the wing drag (mostly induced drag), but slightly decreased the rotor propulsive efficiency. When the rotor moved to the wing tip (C6) for the increased wingspan (C5), wing drag was reduced due to increased beneficial interference effects.

Quad Tilt-Rotor

Performance results for the quad tilt-rotor configuration are discussed in this section. Figures 13–15 show the interference effects on the front and rear wings at the design cruise condition of 300 kt. The interference velocity from the rotors on the wings is shown in Fig. 13. Again, the interference varied with rotor azimuth and exhibited a 4/rev variation due to the four-bladed rotors. The interference on the front wing is similar to that of a conventional tilt-rotor. The maximum interference on the front wing was observed at a 30 deg azimuth angle, at which the blade tip vortex of the rotor passes the wing quarter chord line. The interference velocity values on the front wing are mostly positive due to positive interference velocities from the rear wing. The interference on the rear wing is very complicated because several sources affect it. The most dominant influence comes from the front wing and determines the W-shape distribution. The two humps at ± 0.25 originate from the two rear rotors. These interference velocities reduce the total induced velocity along the front wingspan and significantly increase the total induced velocity along the rear wingspan, as shown in Fig. 14. Even without interference, the induced-velocity distribution of the rear wing is somewhat different from the front wing because of the increased chord near the midspan. The interference has a beneficial effect on the front wing performance, but degrades the rear wing performance, as shown in Fig. 15. The interference effect did not change wing profile power.

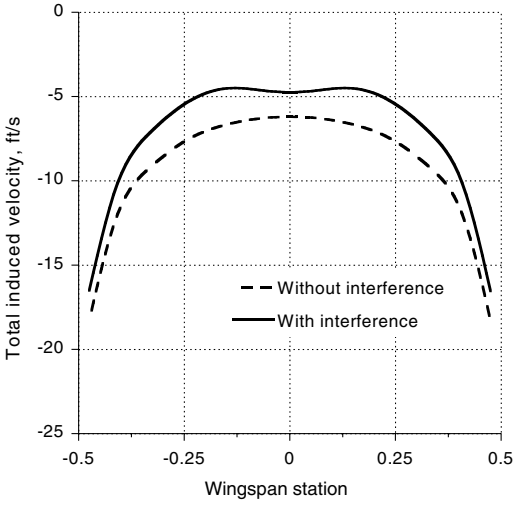

a) Front wing

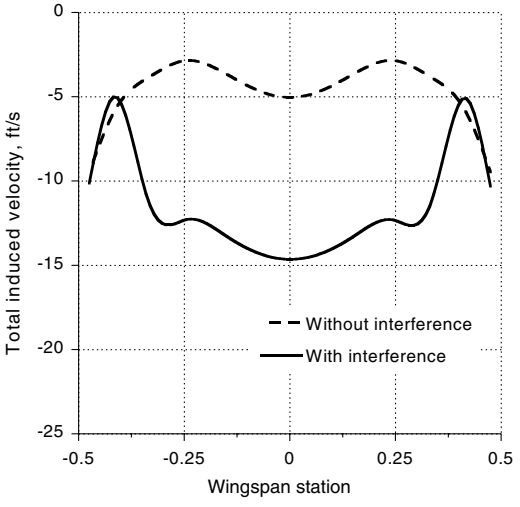

b) Rear wing

Fig. 14 Total induced velocity on the wing of the quad tilt-rotor (positive upward).

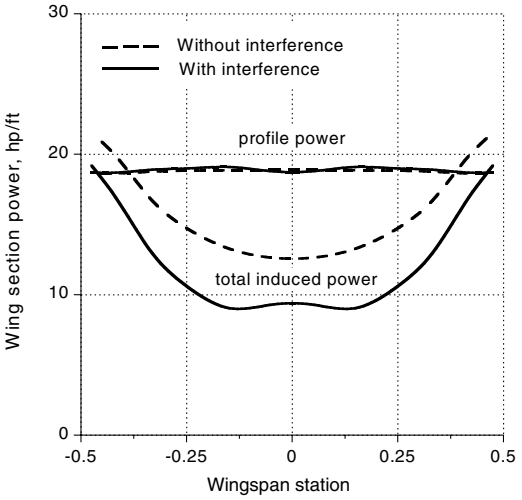

a) Front wing

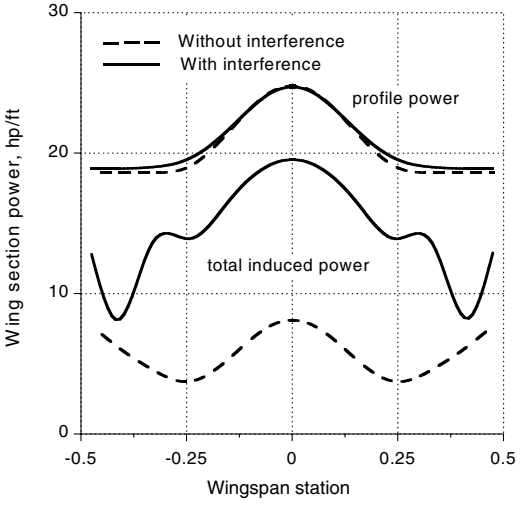

b) Rear wing

Fig. 15 Wing section power of quad tilt-rotor.

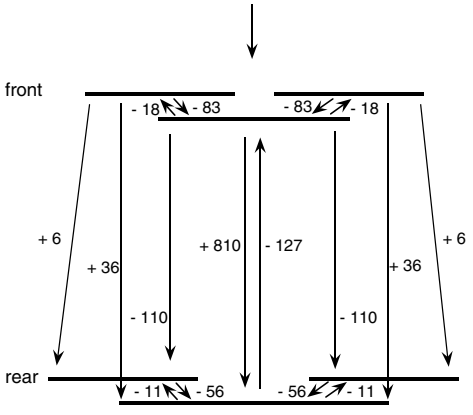

Fig. 16 Interference effect on required power of the quad tilt-rotor; dimensions are in horsepower.

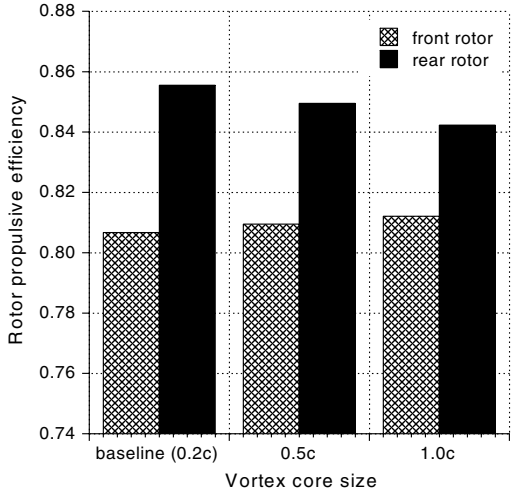

a) Rotor propulsive efficiency

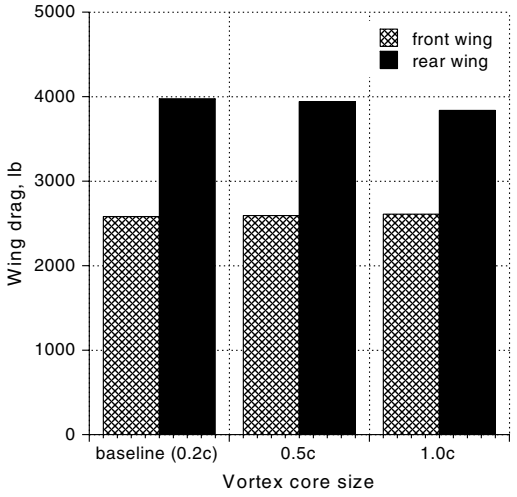

b) Wing drag

Fig. 17 Effects of vortex core size on aircraft performance.

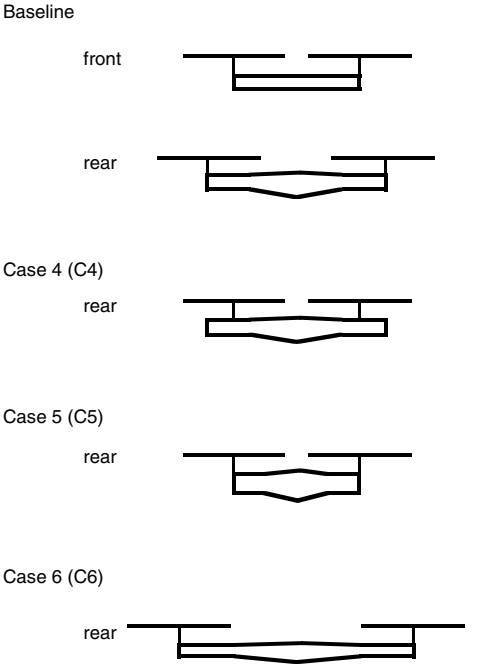

Fig. 18 Rear rotor and wing geometry variations for the quad tilt-rotor.

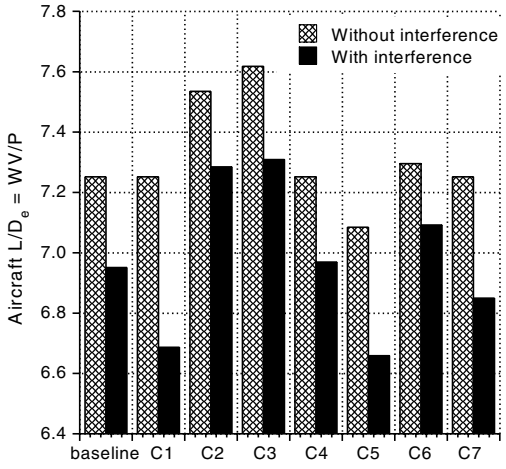

Fig. 19 Aircraft lift-to-drag ratio of the quad tilt-rotor.

Figure 16 quantifies the interference effect on the aircraft cruise performance for the baseline configuration. The required power changes due to interference are shown. The arrows indicate the direction of interference, and the numbers next to the arrows represent the changes in required power due to interference. Positive numbers mean unfavorable interference, and negative numbers beneficial interference. For example, the +6 next to the arrow from "front" to "rear" means that the rear left rotor requires additional 6 hp due to interference from the front left rotor. The interference effects between the front rotors and the front wing and between the rear rotors and the rear wing reduce required power. The front wing has a beneficial influence on the rear rotor power. The rear wing also has a beneficial influence on the front wing (positive interference velocity reduced total induced velocity and, thus, reduced wing induced power). The front rotors increase both the rear rotor power and rear wing power, although the effect is not significant. The most dominant effect is from the front wing to the rear wing. It increases the required power of the rear wing by 810 hp (negative interference velocity increased total induced velocity and, thus, increased wing induced power at most of the wingspan) and, thus, increases the aircraft total required power.

As the vortex core size grows with time (wake age) due to viscous diffusion, the effects of vortex core size on the aircraft performance was investigated. It should be noted that the constant vortex core radius of 20% chord ($0.2c$) was used for all the calculations shown in this paper. Without knowing an accurate core growth rate, a simple way to examine the effect of core growth is to use a larger core size for

Table 4 Parametric variations of quad tilt-rotor

Case 1 (C1)	Change of rotor rotational direction
Case 2 (C2)	Reduction in cruise rotor tip speed to 350 ft/s
Case 3 (C3)	Reduction in wing chord to obtain wing loading of 100 lb/ft^2
Case 4 (C4)	Rear rotors moved inboard to make them directly behind front rotors
Case 5 (C5)	Rear rotors moved inboard and rear wingspan decreased to match front wingspan
Case 6 (C6)	Increase in rear wingspan by 20% and rear rotors moved to the wing tip
Case 7 (C7)	Rear rotors and wings moved down to the same height as front rotors and wings

both rotors and wings when the interference velocity is calculated. Figure 17 shows the effects of vortex core size on the rotor propulsive efficiency and wing drag. The calculations were made with two vortex core sizes (0.5 and 1.0c), and the results are compared with the baseline values. As the vortex core size increases, the front rotor propulsive efficiency increases and the rear wing drag decreases. However, the rear rotor propulsive efficiency decreases and the front wing drag slightly increases at the same time. Thus, the total effect of changing the vortex core size on the aircraft performance is negligible.

A parametric study was conducted to understand the effects of design parameters on the performance of the aircraft. Table 4 shows the design parameters investigated, and the rear rotor and wing geometry variations are illustrated in Fig. 18. The first case was the change of rotor rotational direction. The second case was the reduction in cruise tip speed for all four rotors, to increase the propulsive efficiency of the rotor. The third case was reduction in both front and rear wing chords to obtain a wing loading of $W/S = 100$ lb/ft^2, which is the value for the conventional tilt-rotor. In this case, the wingspan was maintained the same as the baseline value. The fourth case was rear rotors moved inboard to make them directly behind the front rotors. The fifth case was rear rotors moved inboard as in the fourth case, but the rear wingspan decreased to match front wingspan (from 102.6 to 73.3 ft). To maintain the same wing loading, the wing chord was increased accordingly. The sixth case was an increase in the rear wingspan by 20% (from 102.6 to 123.1 ft) and rear rotors moved to the wing tip. To maintain the same wing loading, the wing chord was decreased accordingly. The seventh case was the rear rotors and wings moved down to the same height as the front rotors and wings (baseline separation is 5.02 ft).

Figure 19 shows the performance results in terms of aircraft lift-to-drag ratio $L/D_e = WV/P$, calculated without accessory or other losses, all for the design cruise condition of 300 kt. The performance was calculated using nonuniform inflow with prescribed wake geometry. Rotor/rotor, rotor/wing, and wing/wing interference was accounted for by using a vortex wake model for both the rotors and the wings, and the performance results with interference effects are compared with those without interference effects. Zero flapping trim was used for all the results for the quad tilt-rotor. The interference effects changed the aircraft lift-to-drag ratio by up to 7.8% for the parametric variations investigated. The reduction in rotor tip speed (C2) and increase in wing loading (C3) increased the aircraft lift-to-drag ratio the most, and the increase in rear wingspan (C6 compared with C5) also has a beneficial effect. The change of rotor rotational direction (C1) and the move of the rear rotors and wings to the same height as the front rotors and wings (C7) decreased the aircraft lift-to-drag ratio significantly, and these effects can only be observed with interference included in the calculation. The move of the front rotors inboard (C4) has a negligible influence on the aircraft lift-to-drag ratio; however, the reduction in rear wingspan (C5) significantly reduced the aircraft lift-to-drag ratio.

Figures 20 and 21 show the rotor propulsive efficiency and wing drag, respectively. These are the same calculations as in Fig. 19, except that individual performance components are compared. For the baseline case, there is a reduction in the front-wing induced drag and a significant increase in the rear-wing induced drag because of the nonuniform flowfield from the rotor and wing interference and a

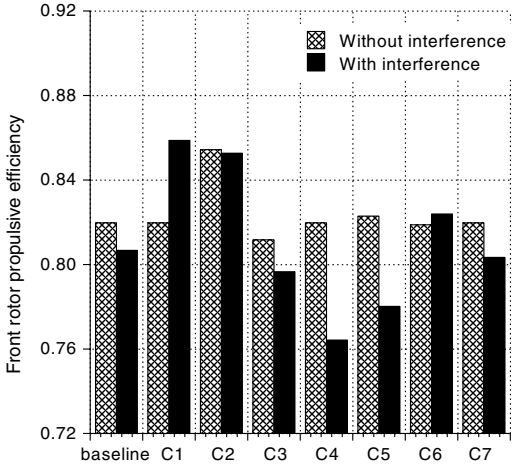

a) Front rotor

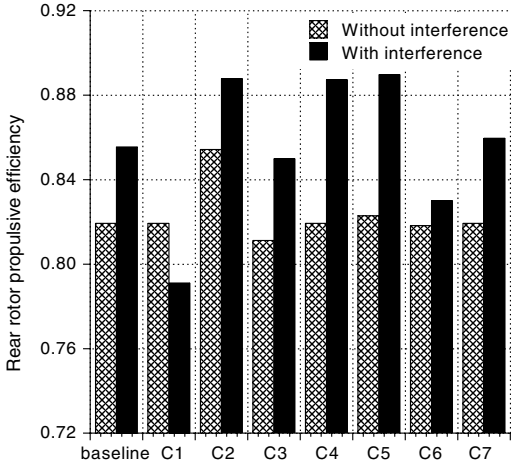

b) Rear rotor

Fig. 20 Rotor propulsive efficiency of the quad tilt-rotor.

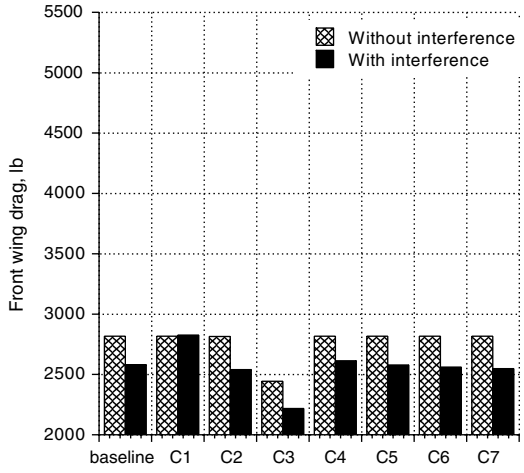

a) Front wing

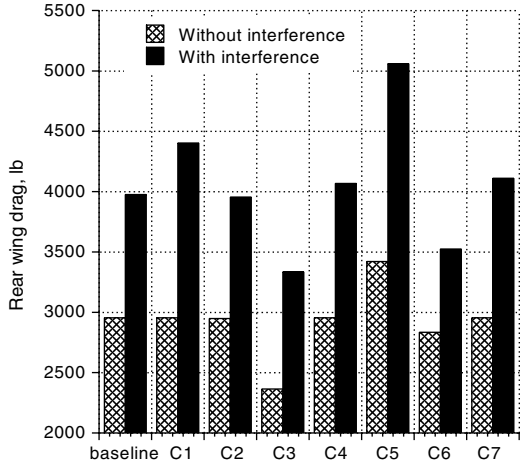

b) Rear wing

Fig. 21 Wing drag of the quad tilt-rotor.

slight reduction in the front rotor propulsive efficiency and an increase in rear rotor propulsive efficiency because of the combination of the interference and the front rotor thrust decrease and rear rotor thrust increase. The change of rotor rotational direction (C1) increased the front rotor propulsive efficiency. However, it also increased the wing drag significantly; thus, an overall performance penalty was observed. The reduction in rotor tip speed (C2) increased the rotor propulsive efficiency as well as decreased the wing drag. Thus, the most performance improvement was obtained. The increase in wingspan (C6 compared with C5) decreased the wing drag, but slightly decreased the rotor propulsive efficiency.

Without interference effect, the front wing drag values did not change with the parametric variations except for the wing loading change (C3). With interference effect, the change of rotor rotational direction (C1) increased the front wing drag significantly, as for the conventional tilt-rotor. The increase in wing loading (C3, wing chord was reduced with same span as baseline) significantly reduced the front wing drag. The significant drag reduction came from profile drag reduction due to the reduced chord. However, induced drag slightly increased.

The rear wing drag values showed significant variations with the parametric variations, and the rear wing drag values always increased with the interference effects for the parametric variations investigated. The biggest penalty came from the reduction in the rear wingspan (C5) due to the increased induced and interference drag. The biggest benefit came from the increase in wing loading (C3) and the increase in the rear wingspan (C6 compared with C5). However, the reasons for the wing performance improvement are different. The increase in wing loading (C3) resulted in the reduction in profile drag, but the increase in the rear wingspan (C5) resulted in the reduction in induced and interference drag.

Conclusions

A performance and design investigation was conduced for 146,600 lb conventional and quad tilt-rotors, which are to cruise at 300 kt at a 4000 ft/95°F condition. The aerodynamic interference effects were included in the comprehensive calculations to better understand the physics and to quantify the effects on the aircraft design.

From this study, the following conclusions were obtained.

Conventional tilt-rotor

1) Interference effect improves the aircraft lift-to-drag ratio of the baseline conventional tilt-rotor. The interference velocities reduce the total induced velocity along the wingspan and, thus, reduce wing induced power.

2) The reduction in rotor tip speed increased the aircraft lift-to-drag ratio the most among the design parameters investigated, and the increase in wingspan also has a beneficial effect on aircraft performance.

3) The change of rotor rotational direction decreased the aircraft lift-to-drag ratio significantly, and this effect can only be observed with interference included in the calculation.

Quad tilt-rotor

1) Interference effect degrades the aircraft performance of the baseline quad tilt-rotor. The most dominant unfavorable effect is from the front wing to the rear wing; it increases the rear wing total induced power significantly and, thus, decreases the aircraft lift-to-drag ratio.

2) The reduction in rotor tip speed and increase in wing loading increased the aircraft lift-to-drag ratio the most among the design parameters investigated.

3) The change of rotor rotational direction decreased the aircraft lift-to-drag ratio significantly, and this effect can only be observed with interference included in the calculation.

References

[1] Johnson, W., Yamauchi, G. K., and Watts, M. E., "Design and Technology Requirements for Civil Heavy Lift Rotorcraft," *Proceedings of the American Helicopter Society Vertical Lift Aircraft Design Conference*, American Helicopter Society, Alexandria, VA, Jan. 2006.

[2] Felker, F. F., Maisel, M. D., and Betzina, M. D., "Full-Scale Tilt-Rotor Hover Performance," *Journal of the American Helicopter Society*, Vol. 31, No. 2, April 1986, pp. 10–18.

[3] Felker, F. F., and Light, J. S., "Aerodynamic Interactions Between a Rotor and Wing in Hover," *Journal of the American Helicopter Society*, Vol. 33, No. 2, April 1988, pp. 53–61. doi:10.4050/JAHS.33.53

[4] Wood, T. L., and Peryea, M. A., "Reduction of Tiltrotor Download," *Journal of the American Helicopter Society*, Vol. 40, No. 3, July 1995, pp. 42–51. doi:10.4050/JAHS.40.42

[5] McVeigh, M. A., Grauer, W. K., and Paisley, D. J., "Rotor/Airframe Interactions on Tiltrotor Aircraft," *Journal of the American Helicopter Society*, Vol. 35, No. 3, July 1990, pp. 43–51. doi:10.4050/JAHS.35.43

[6] Snyder, D., "The Quad Tiltrotor: Its Beginning and Evolution," *Proceedings of the American Helicopter Society 56th Annual Forum*, American Helicopter Society, Alexandria, VA, May 2000, pp. 48–61.

[7] Radhakrishnan, A., and Schmitz, F. H., "An Experimental Investigation of a Quad Tilt Rotor in Ground Effect," AIAA Paper 2003-3517, June 2003.

[8] Radhakrishnan, A., and Schmitz, F. H., "Quad Tilt Rotor Download and Power Measurements in Ground Effect," AIAA Paper 2006-3471, June 2006.

[9] Gupta, V., and Baeder, J. D., "Quad Tiltrotor Aerodynamics in Ground Effect," *Proceedings of the American Helicopter Society 58th Annual Forum*, American Helicopter Society, Alexandria, VA, June 2002.

[10] Gupta, V., and Baeder, J. D., "Investigation of Quad Tiltrotor Aerodynamics in Forward Flight Using CFD," AIAA Paper 2002-2812, June 2002.

[11] Preston, J., and Peyran, R., "Linking a Solid-Modeling Capability with a Conceptual Rotorcraft Sizing Code," *Proceedings of the American Helicopter Society Vertical Lift Aircraft Design Conference*, American Helicopter Society, Alexandria, VA, Jan. 2000.

[12] Johnson, W., "Technology Drivers in the Development of CAMRAD II," American Helicopter Society Paper PS.3 Jan. 1994.

[13] Johnson, W., "Calculation of Tilt Rotor Aeroacoustic Model (TRAM DNW) Performance, Airloads, and Structural Loads," *Proceedings of the American Helicopter Society Aeromechanics Specialists' Meeting*, American Helicopter Society, Alexandria, VA, Nov. 2000.

[14] Potsdam, M., Yeo, H., and Johnson, W., "Rotor Airloads Prediction Using Loose Aerodynamic/Structural Coupling," *Journal of Aircraft*, Vol. 43, No. 3, May–June 2006, pp. 732–742. doi:10.2514/1.14006

[15] Drees, J. M., "Prepare for the 21st Century—The 1987 Alexander A. Nikolsky Lecture," *Journal of the American Helicopter Society*, Vol. 32, No. 3, July 1987, pp. 3–14.